Korean Journal of Chemical Engineering
https://doi.org/10.1007/s11814-024-00278-z

ORIGINAL ARTICLE

Improving Quantum Dot Stability Against Heat and Moisture with Cyclic Olefin Copolymer Matrix

Seon Hui Baek[1,2] · Seung Jae Kim[1] · Ho Seok Heo[1] · Kangtaek Lee[1]

Received: 23 April 2024 / Revised: 4 August 2024 / Accepted: 5 September 2024

Abstract

Quantum dots (QDs) are widely studied for their superior optical properties. However, maintaining their stability requires effective protection against heat and moisture. This research aims to enhance the stability of QDs by embedding them in cyclic olefin copolymer (COC). Our findings show that nanocomposites containing green- and red-emitting QDs in COC exhibited enhanced transparency and dispersion when compared to those using other common polymers, such as polydimethylsiloxane (PDMS) and poly(methyl methacrylate) (PMMA). Stability test under harsh conditions (85 °C and 85% relative humidity) confirmed the robustness of the QDs within the COC matrix compared to the PDMS and PMMA matrices. In addition, a white-light-emitting diode (LED) device was successfully fabricated by integrating a blend of green- and red-emitting QDs in COC-based nanocomposites atop a blue LED chip. This setup demonstrated potential for use in light-emitting devices that demand high luminous efficiency and transparency, even under extreme conditions. The study highlights the potential of COC as an alternative to traditional polymers, enhancing the performance and durability in display technologies.

Keywords Quantum dot · Cyclic olefin copolymer · Stability · Light-emitting diode · Display

Introduction

Quantum dots (QDs) are nano-sized semiconductor particles whose emission wavelength can be finely tuned by adjusting their size during synthesis, owing to the quantum confinement effect. These QDs also possess other remarkable optical properties, such as high color purity and photoluminescence quantum yield (PLQY), wide absorption and emission spectra, and high photostability [1]. Due to these characteristics, quantum dots have been widely studied and employed in modern display technologies [2–4].

Despite their exceptional optical properties, protecting QDs from heat and moisture is crucial to ensure their stability and reliability in their applications, as they remain susceptible to environmental factors [5]. Exposure to moisture can trap excited electrons on the QD surface, leading to a decrease in PLQY and a redshift in the emission spectrum [6–9]. Likewise, high temperatures can impair the optical properties of QDs, causing a redshift, increased full width at half maximum (FWHM), and reduced PLQY due to exciton-photon scattering [10]. To enhance the stability of QDs, various strategies have been pursued. Notably, embedding QDs within a polymer matrix has proven particularly effective in protecting them from heat and moisture. This method also allows for precise management of their electronic and optical properties while maintaining the mechanical features of the polymer matrix.

Polydimethylsiloxane (PDMS) and poly(methyl methacrylate) (PMMA) are two transparent polymers frequently used to disperse QDs, but they have limitations due to their poor physical properties. Specifically, encapsulating QDs in PMMA can significantly reduce the quantum efficiency (QE) of the resulting nanocomposite. This decrease is often attributed to PMMA's low thermal stability and limited resistance to water [11]. Furthermore, during the manufacturing process of QD-polymer nanocomposites, QDs may aggregate due to the van der Waals interaction between the

Seon Hui Baek and Seung Jae Kim these authors equally contributed to this work.

✉ Kangtaek Lee
ktlee@yonsei.ac.kr

[1] Department of Chemical and Biomolecular Engineering, Yonsei University, Seodaemun-Gu, Seoul 03722, Republic of Korea

[2] Display Research Center, Samsung Display Co., Giheung-Gu, Yongin-Si, Gyeonggi-Do 17113, Republic of Korea

Published online: 18 September 2024

QDs. This aggregation triggers unwanted energy transfer and reabsorption events among the QDs, which reduce the QE [12]. To enhance the performance of QD-based devices, it is crucial to ensure a uniform distribution of QDs within the polymer matrix.

In this work, we present enhancing the stability of QD-polymer nanocomposites by integrating QDs into cyclic olefin copolymer (COC). COC was selected due to its low water absorption rate, high resistance to polar solvents, and superior optical transmittance compared to PDMS and PMMA [13, 14]. In addition, the moisture permeability of COC is significantly lower than that of PMMA and PDMS [15, 16], making it an ideal material for protecting QDs from environments. We developed QD/COC nanocomposites characterized by high transparency, low moisture permeability, and improved thermal stability. Our results indicate that COC outperforms both PDMS and PMMA in optical properties and thermal stability, demonstrating its effectiveness in enhancing the stability of QDs for use in display technologies.

Experimental

Materials

Zinc acetate ($Zn(OAc)_2$), indium acetate ($In(OAc)_3$), myristic acid, oleic acid (OA), zinc acetate dihydrate ($Zn(OAc)_2{\cdot}2H_2O$), 1-octadecene (ODE), zinc chloride ($ZnCl_2$), indium chloride ($InCl_3$), oleylamine (OLA), sulfur (S), tri-octyl phosphine (TOP), selenium (Se), tris(dimethylamino) phosphine ($P(DMA)_3$), poly(methyl methacrylate) (PMMA) and 1-dodecanethiol (DDT) were purchased from Aldrich. Tris(trimethylsilyl)phosphine ($(TMS)_3P$) was purchased from JSI Silicone. Polydimethylsiloxane (Sylgard 184, PDMS) was purchased from Dow Corning. Gallium trichloride ($GaCl_3$) was purchased from Strem Chemicals Inc. Chloroform, 1,2-dichlorobenzene (O-DCB), ethyl alcohol, and n-hexane were purchased from Daejung Chemicals. COC was purchased from GFM.

Synthesis of Green- and Red-Emitting QDs

Green-emitting InP/GaP/ZnS QDs were synthesized according to the literature [17]. $In(OAc)_3$ (0.24 mmol), myristic acid (2.17 mmol), ODE (4 mL), and $Zn(OAc)_2$ (1 mmol) were mixed in a 50 mL three-neck flask. The mixture was heated to 110 °C under gentle stirring and degassed for 2 h under vacuum. After degassing, the mixture was purged with Ar gas. The mixture was heated to 270 °C and rapidly cooled to 25 °C. $(TMS)_3P$ (0.29 mmol) dissolved in ODE (1 mL) and $GaCl_3$ (0.085 mmol) dissolved in ODE (1 mL) were added to the mixture, and it was heated to 300 °C and reacted for 90 s. Then, 1-DDT (0.25 mL) was injected into the mixture and maintained for 10 min at 300 °C. Zinc oleate (2 mmol) prepared by mixing $Zn(OAc)_2$ (2 mmol), OA (1.26 mL), and ODE (1.5 mL) was additionally added to the solution. Then, 1-DDT (0.75 mL) was immediately injected into the mixture and reacted at 300 °C for 10 min. After the reaction, the mixture was cooled to room temperature, and washed by centrifugation (9000 rpm, 10 min) using ethanol/hexane mixture. The synthesized InP/GaP/ZnS QDs were dispersed in chloroform and stored in a refrigerator.

Red-emitting InP/ZnSeS/ZnS QDs were synthesized according to the literature [18]. $InCl_3$ (0.45 mmol), $ZnCl_2$ (2.2 mmol) and OLA (6 mL) were mixed in a 50 mL three-neck flask. The mixture was heated to 120 °C under gentle stirring and degassed for 1 h under vacuum. After degassing, the mixture was purged with Ar gas and heated to 180 °C for 30 min. After heating, $P(DMA)_3$ (0.19 mmol) was rapidly injected into the mixture and reacted at 180 °C for 30 min. Se stock solution with Se (0.12 mmol) in TOP (1 mL) was slowly injected to the mixture and reacted at 200 °C for 30 min. Zn stock solution mixed with zinc stearate (1.58 mmol) and ODE (4 mL) was slowly injected to the mixture and reacted at 220 °C for 30 min. The Se-S stock solution containing Se (0.06 mmol), S (2 mmol), and TOP (1.6 mL) was slowly added to the mixture at 240 °C and maintained for 30 min. Subsequently, the identical Zn stock solution that was used previously was injected slowly at 260 ℃ and maintained for 30 min. Following this, the S-rich stock solution (0.02 mmol Se and 4 mmol S in 2 mL TOP) was injected slowly at 280 ℃ and maintained at that temperature for 30 min. Then, the same amount of Zn stock solution was additionally added at 300 °C, and reacted for 60 min. After the reaction, 1-DDT (5 mL) was slowly injected and reacted at 200 °C for 60 min. Then, zinc oleate (3.3 mL) with zinc acetate (3 mmol) and OA (6 mL) were added into the mixture and reacted at 190 °C for 120 min. After 120 min, the mixture was cooled to room temperature and washed by centrifugation (9000 rpm, 10 min) using ethanol/hexane mixture. The synthesized InP/ZnSeS/ZnS QDs were dispersed in chloroform and stored in a refrigerator.

Fabrication of QD/COC Nanocomposite and White LED Device

To prepare QD/COC nanocomposite, polymer solution was prepared by dissolving 300 mg of COC in 0.9 mL of O-DCB. Red- or green-emitting QDs in chloroform were mixed with the polymer solution at room temperature. The mixture containing 1 wt% QDs was coated onto a glass substrate (25 mm × 25 mm) via solvent casting, followed by overnight drying at room temperature (Scheme 1). For a comparison, PMMA or PDMS was also used as a polymer matrix for nanocomposites.

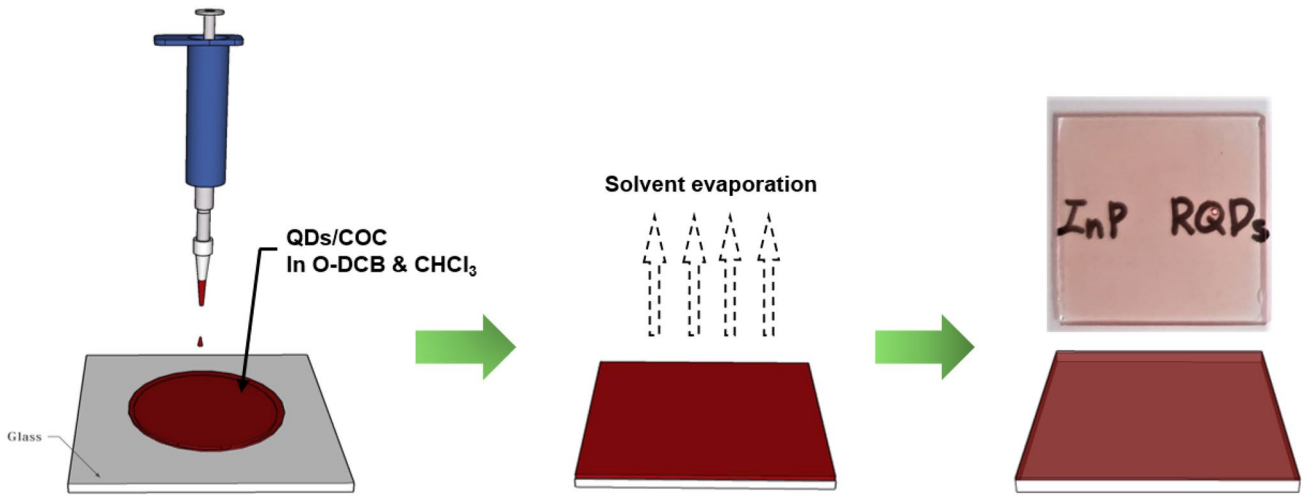

Scheme 1. Schematic illustration of the fabrication of red-emitting QD/COC nanocomposite

The QD/PMMA nanocomposite was fabricated using an identical procedure to that used for the QD/COC nanocomposite while QD/PDMS nanocomposite was prepared by curing at 110 °C for 90 min.

The white LED device was fabricated by using a QD/COC nanocomposite. In the fabrication process, green- and red-emitting QDs were employed to convert the blue light emitted by the LED chip. This involved blending a COC solution in O-DCB with the QDs dispersed in chloroform, leading to the formation of the QD/COC nanocomposite. The composition of the green-emitting QDs to red-emitting QDs in the COC was 8:1 in wt%. The mixture was applied onto the surface of a blue LED chip (Dae-Kwang Illumination $\lambda_{ex} = 450$ nm) [19] and left to dry overnight.

Characterization

The UV–vis absorption spectra of the QDs and the transmittance of the nanocomposite films were acquired using a spectrophotometer (V-730, JASCO). The quasi-elastic light scattering (QELS, Nano-ZS ZEN 3600, Malvern) was used to measure the average hydrodynamic diameter of the QDs. The dispersion states of QDs within the nanocomposite were analyzed using a confocal microscope (LSM 880, Carl Zeiss). The QE of both QDs and the nanocomposite was assessed employing a spectrofluorometer (FP-8500, Jasco) in conjunction with an integrating sphere (ILF-835, JASCO). The LED-correlated color temperature (CCT) of the LEDs was determined by employing an integrating sphere of a spectrofluorometer (QE-1000, Otsuka Electronics) with a 450 nm xenon (Xe) laser as an excitation energy source.

Results and Discussion

Optical characteristics of QD/COC nanocomposites

The PL and UV absorption spectra of the synthesized green-emitting InP/GaP/ZnS QDs and red-emitting InP/ZnSeS/ZnS QDs exhibited first excitonic absorption peaks at 478 nm and 576 nm and emission peaks at 525.5 nm and 613 nm, respectively (Fig. 1 (a) and (b)). In addition, the average hydrodynamic diameters of the green-emitting and red-emitting QDs, as determined by QELS, were 8.2 nm and 8.9 nm, respectively.

The synthesized QDs were then mixed with COC to fabricate QD/COC nanocomposite films. For a comparison, PMMA and PDMS were also used as matrix polymers in the fabrication of nanocomposite films. To investigate the relation between the optical properties and the dispersion states of QDs within different polymer matrices, the absorption and PL spectra of the nanocomposites were recorded. Analysis of the PL spectra revealed a redshift in the emission peaks of QD nanocomposites. Specifically, for green-emitting QDs, the redshifts were 18.7 nm, 32.1 nm, and 37.1 nm for QD/COC, QD/PMMA, and QD/PDMS nanocomposites, respectively (Fig. 2(a)). For red-emitting QDs, the redshifts were 14.1 nm, 27.8 nm, and 28 nm for QD/COC, QD/PMMA, and QD/PDMS, respectively (Fig. 2(b)). Among these, QD/COC composites exhibited the smallest redshift for both types of QDs. When QDs aggregate, strong electronic coupling between neighboring QDs causes hybridization of band edge orbitals, leading to a redshift in the PL spectra. In addition, exciton energy transfer from larger bandgap QDs to adjacent smaller bandgap QDs results in a redshift of the emission peak. Aggregation of QDs also leads to increased light scattering, decreased transmittance,

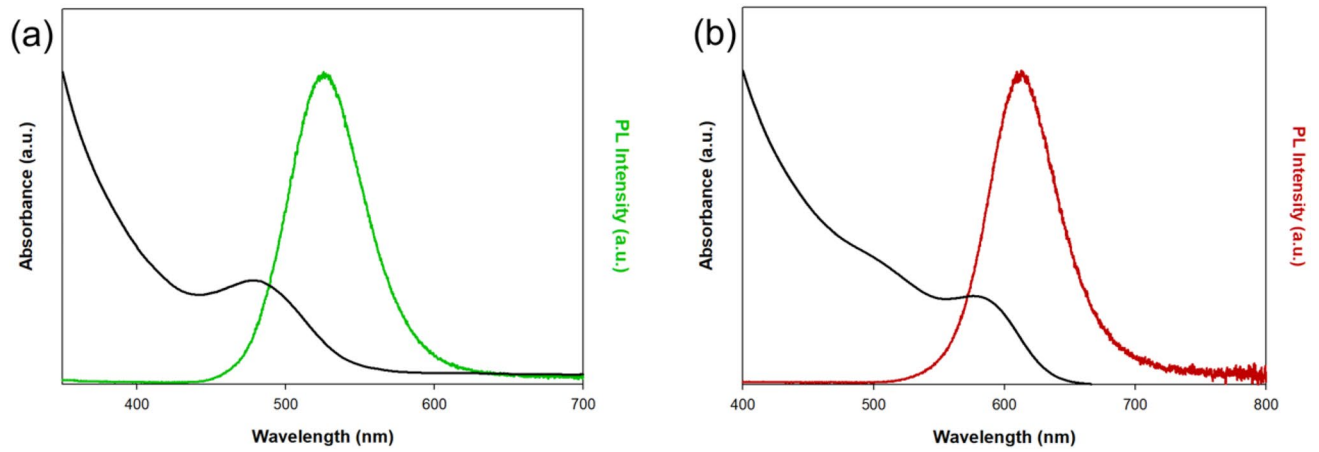

Fig. 1 Absorption and PL spectra of **a** green-emitting InP/GaP/ZnS QDs and **b** red-emitting InP/ZnSeS/ZnS QDs

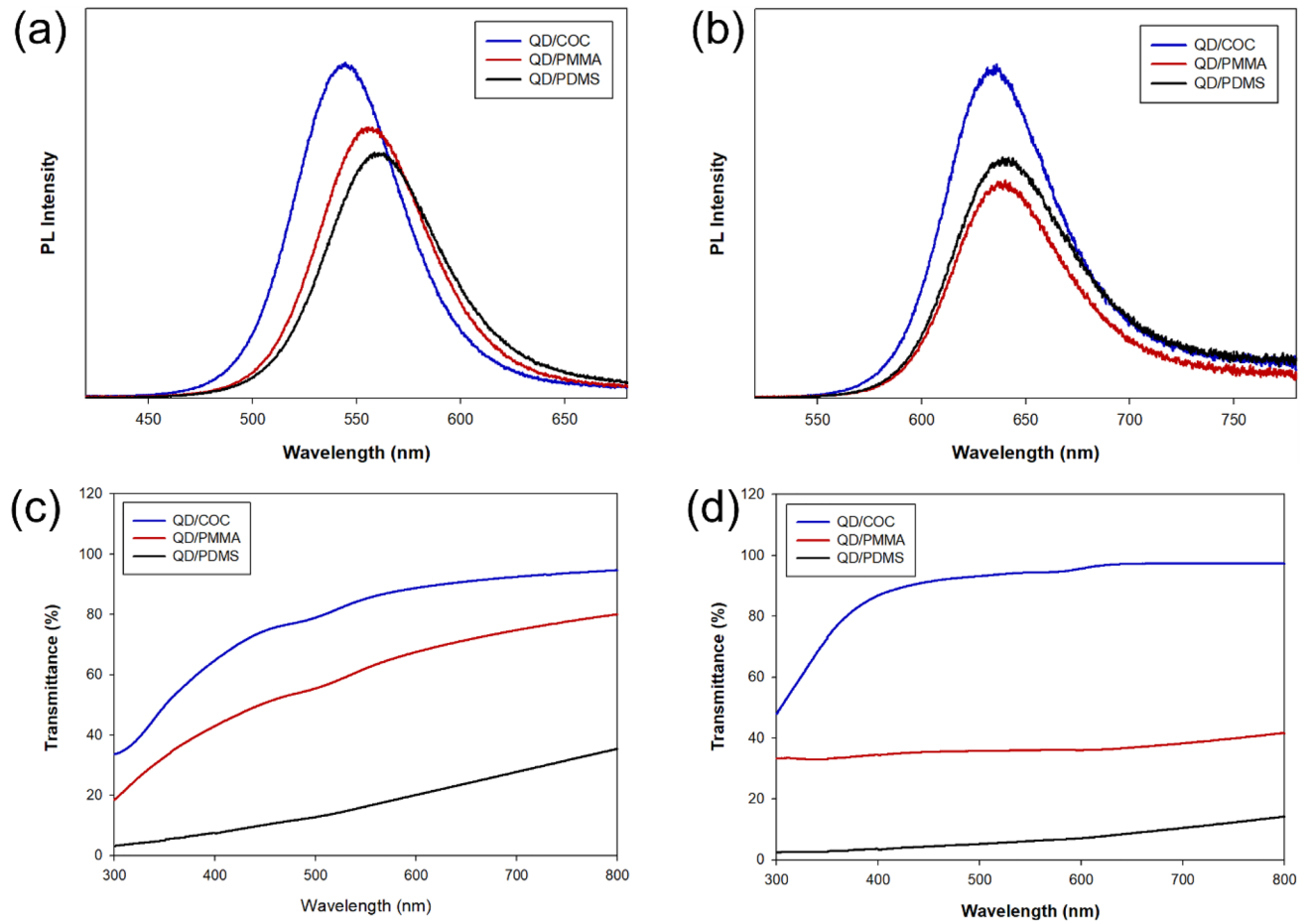

Fig. 2 PL spectra and transmittance of (**a**, **c**) green-emitting and (**b**, **d**) red-emitting QD/polymer nanocomposites

and reabsorption of light within the nanocomposites, thereby reducing PL intensity [20–24]. To further substantiate this theory, the transmittances of the nanocomposites were measured. The results, in Figs. 2(c) and (d), demonstrated that QD/COC nanocomposites had significantly higher transmittance than QD/PMMA and QD/PDMS nanocomposites. This indicates that a more uniform dispersion of QDs within the COC matrix results in higher transmittance, stronger PL

intensity, and a reduced redshift, in contrast to the aggregated QD/PMMA and QD/PDMS matrices.

When polymers display low compatibility with QDs, this often leads to QD aggregation or phase separation, adversely affecting efficiency. Such QD aggregation, marked by reduced transmittance and observable redshift, can be visually detected. Assessing the dispersion of nanocomposites with a 1 wt% QD concentration under daylight revealed that QD/COC appeared as a transparent film without QD aggregates, whereas QD/PDMS and QD/PMMA displayed noticeable aggregates and opacity, as shown in Fig. 3. Under UV light, the superior dispersion of QD/COC nanocomposites was also evident, showcasing uniform dispersion without aggregation, unlike QD/PDMS and QD/PMMA. This highlights the critical role of polymer-QD compatibility in ensuring uniform dispersion and preventing aggregation.

Further evaluation of QD dispersion within the nanocomposites was conducted using confocal microscopy, with results consistent with the daylight and UV light observations, as shown in Fig. 3. In QD/COC, QDs were evenly dispersed without aggregates, while QD/PDMS showed not only aggregation but also voids devoid of QDs. This phenomenon was attributed to the different interactions between the QDs and the polymer matrices. In QD/PMMA and QD/PDMS, the long carbon chains (aliphatic chains) of the QD ligands tended to interact preferentially among themselves than with the polymers, leading to aggregation and the formation of voids. However, in QD/COC, the interaction between aliphatic chains from the QD ligands and ethylene segments from the COC was favorable, promoting a uniform distribution of QDs within the COC matrix. This result illustrates the significance of polymer selection for uniform QD dispersion and aggregation mitigation.

Thermal Stability of QD/COC Nanocomposite

To assess the thermal stability of QD/COC nanocomposites, nanocomposites were exposed to high temperature (85 ℃) in a convection oven for 15 days. Figure 4(a) shows the results for green-emitting QD/COC, QD/PMMA, and QD/PDMS nanocomposites. Over this period, the normalized QE of QD/COC decreased by ~ 14.6%. However, both QD/PMMA and QD/PDMS nanocomposites displayed more significant decrease in normalized QEs. For instance, they exhibited a rapid decrease in normalized QE (by ~ 20% for QD/PMMA and ~ 40% for QD/PDMA) only after 2 days, followed by continued decrease to final QE values of 60% and 55% for QD/PMMA and QD/PDMA after 15 days, respectively. Figure 4(b) shows the results for red-emitting nanocomposites under the same conditions. The normalized QE of the red-emitting nanocomposite showed similar trends as the green-emitting ones: the total decrease in normalized QE after 15 days was by 10.9%, 22.8%, and 58.8% for QD/COC, QD/PMMA, and QD/PDMS nanocomposites, respectively.

To investigate stabilities against both heat and moisture, we performed stability experiments over a 15-day period in a thermo-hygrostat chamber under 85 °C and 85% RH. Figure 5(a) shows that after 15 days, the normalized QE of the QD/COC nanocomposite declined slightly (by ~ 7.3%), which was close to its initial value. In contrast, the normalized QE of the QD/PMMA nanocomposite gradually decreased by ~ 30.9%, while the QD/PDMS nanocomposite

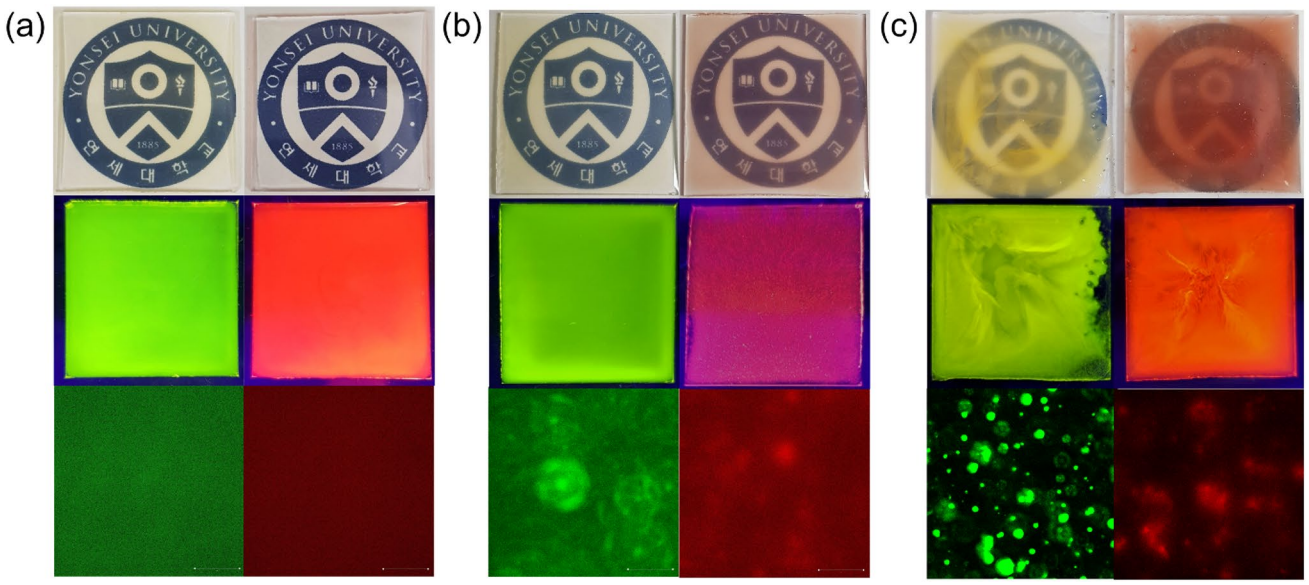

Fig. 3 Images of QD/polymer nanocomposite films under daylight (top) and UV light (middle), and confocal micrographs (bottom): **a** QD/COC, **b** QD/PMMA, **c** QD/PDMS

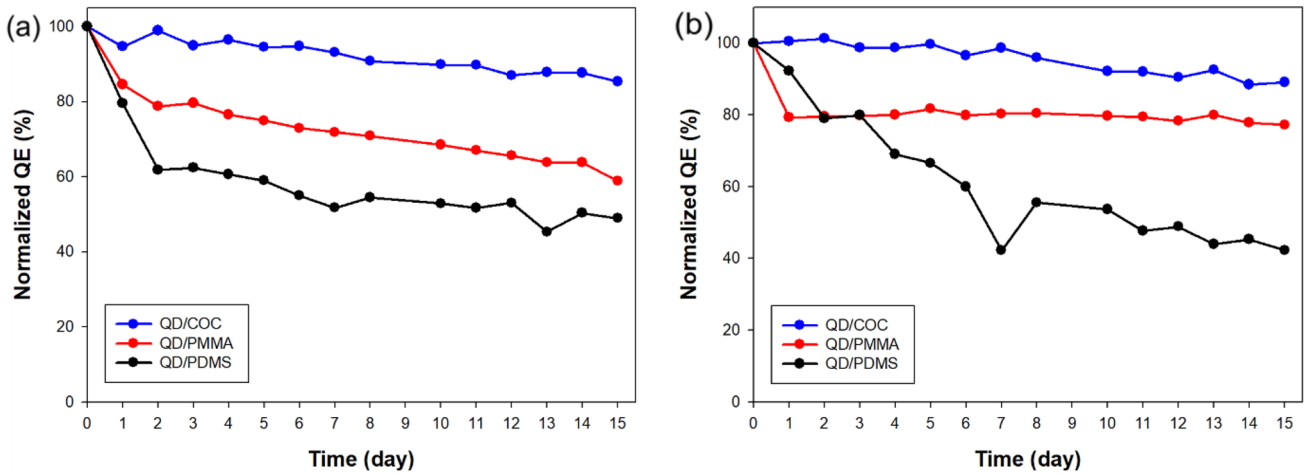

Fig. 4 The normalized QE of **a** green-emitting and **b** red-emitting QD/polymer nanocomposites at 85 ℃

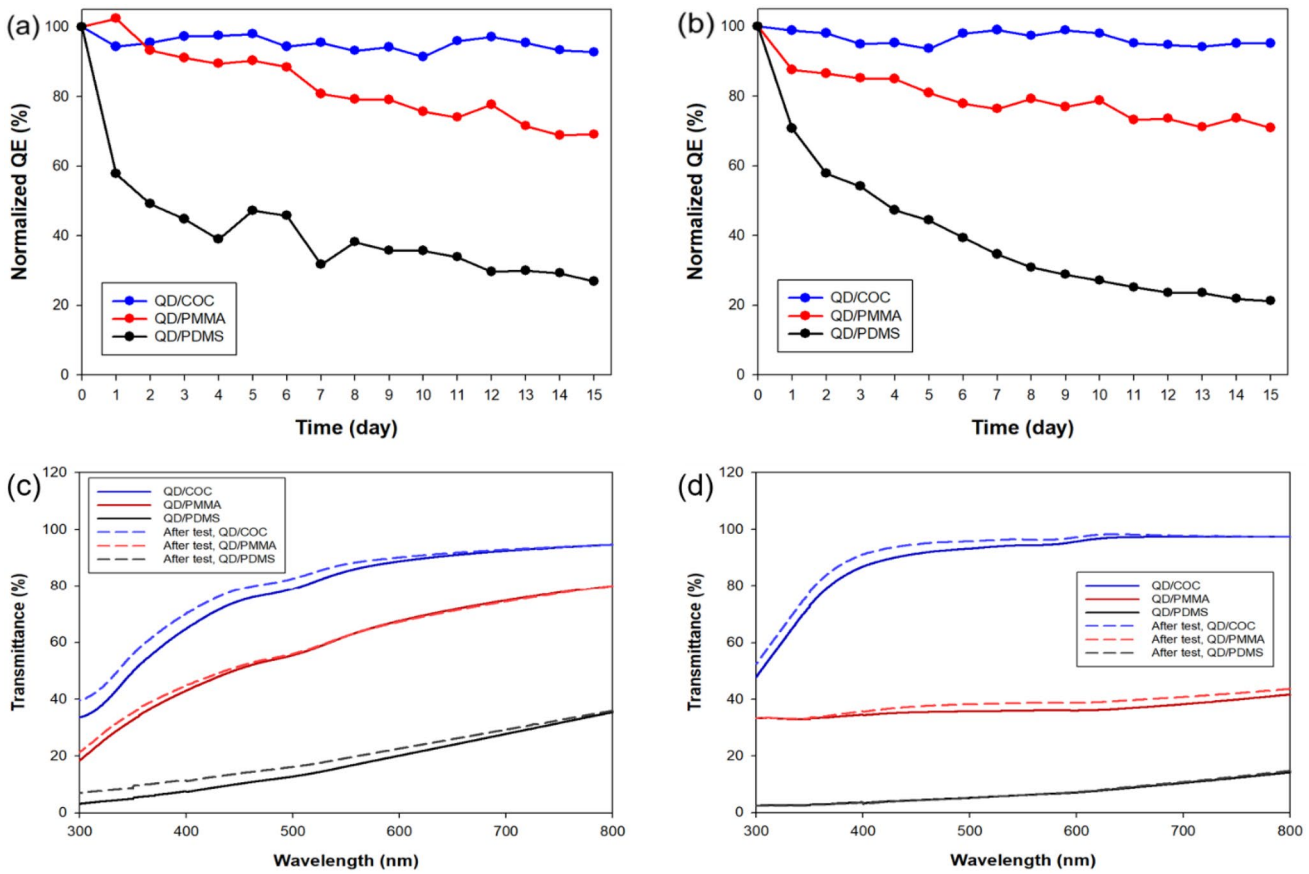

Fig. 5 The normalized QE of **a** green- and **b** red-emitting QD/polymer nanocomposites at 85 ℃/85%RH. The transmittance of **c** green- and **d** red-emitting QD/polymer nanocomposites before and after the stability test

exhibited a more substantial decrease, dropping by ~ 40% within the first two days and then by 73.15% after 15 days. Therefore, the decrease in QE for the COC nanocomposite was significantly lower than those for the PMMA and PDMS nanocomposites. Figure 5(b) demonstrated similar trends for the red-emitting QD/COC, QD/PMMA, and QD/PDMS nanocomposites under identical conditions. After the stability test, a blueshift of the emission peak occurred due

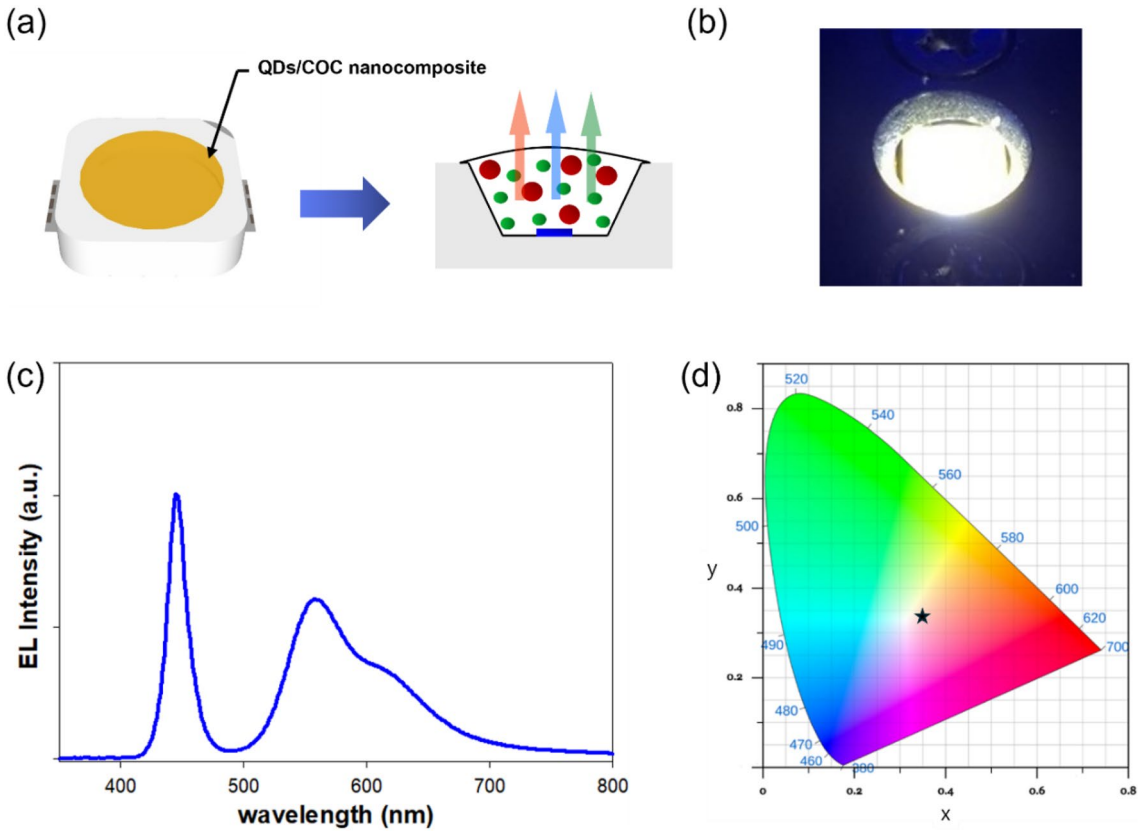

Fig. 6 **a** Schematic illustration of the fabrication of white LED device, and **b** Image of the emitted white light, **c** Electroluminescence spectra and **d** Color coordinates of a white LED device using QD/COC

to a decrease in the QD size [25]. Specifically, for green-emitting QDs, the changes in emission wavelengths were 2.5 nm, 4.7 nm, and 8.4 nm for QD/COC, QD/PMMA, and QD/PDMS nanocomposites, respectively. For red-emitting QDs, the changes in emission wavelengths were 2.3 nm, 4.4 nm, and 7.5 nm for QD/COC, QD/PMMA, and QD/PDMS, respectively. Notably, the QD/COC nanocomposite exhibited the smallest blueshift compared to the QD/PMMA and QD/PDMS nanocomposites.

These findings demonstrate that QD/COC nanocomposites exhibited relatively minor decreases in their properties when subjected to high temperature or high-humidity conditions. The exposure of QDs to elevated temperatures can induce changes in the bandgap due to the coupling effect between exciton electrons and phonons, potentially compromising the optical properties of QDs [8–10, 22, 26–28]. However, QD/COC nanocomposites demonstrated stability against heat and moisture, showing only minor reductions in QE. In comparison, COC displays superior physical characteristics over PMMA and PDMS, notably in its low moisture absorption rate, which enhances its resistance to moisture penetration and helps maintain stable QE. In addition, the production of COC films does not require curing process, reducing their vulnerability to heat-induced deformation, and further preserving QE. These factors highlight the excellent moisture stability of the COC-polymer matrix, significantly contributing to the nanocomposite's overall stability [14, 29]. After the stability test, we measured transmittances of the films to observe changes in their optical properties. As shown in Figs. 5(c) and 5(d), the changes in transmittances were negligible after the stability test.

White LED Devices Utilizing QD/COC Nanocomposite

White LEDs were developed using a QD/COC nanocomposite, and their potential applications were assessed. To fabricate the device, QDs that emit green and red light were used to convert the blue light from the LED chip, as shown in Fig. 6(a). The process involved blending a COC solution in 1,2-dichlorobenzene with green- and red-emitting QDs in chloroform to form the QD/COC nanocomposite. After testing different mixing ratios and considering the reabsorption from green-emitting QDs to red-emitting QDs, the optimal ratio of green to red QDs was determined to be 8:1 in wt%. This mixture was then applied to a blue LED chip and left to dry overnight. Figure 6(b) displays the resulting white-light

emission from the LEDs. The color temperature of this light was quantified using an integrating sphere and a 450 nm Xenon laser, with a recorded value of 4760.9 K. The color coordinate (0.349, 0.333) presented on the CIE chromaticity diagram in Fig. 6(d) confirms the effective production of white light. Furthermore, luminous efficiency, which is the ratio of luminous flux to power measured in lumens per watt in the International System of Units, was measured at 28.2 lm/W. The successful development of these QD-based white LEDs demonstrate their potential not only in generating white light for displays but also in both indoor and outdoor lighting applications [30].

Conclusions

QDs are well known for their excellent optical properties but requires protection from harsh environmental conditions like heat and moisture to maintain their performance and stability. Our research aimed to enhance the stability of QDs by incorporating them into COC. We found that nanocomposites made of green- and red-emitting QDs encapsulated in COC not only demonstrated superior transparency and dispersion but also showed increased resistance to heat and moisture compared to those encapsulated in PMMA and PDMS. Our results introduce a novel approach to fabricating a QD color conversion layer, using COC as the matrix material to improve both performance and durability.

Acknowledgements This work was supported by the National Research Foundation of Korea (NRF) [grant numbers NRF-2018R1A5A1024127 and 2021M3H4A3A01062960].

Funding National Research Foundation of Korea,NRF-2018R1A5A1024127,Kangtaek Lee,NRF-2021M3H4A3A01062960,Kangtaek Lee.

Data availability Data will be made available on request.

Declaration

Conflict of interests There are no conflicts of interest to declare.

References

1. J.C. De Mello, H.F. Wittmann, R.H. Friend, Adv. Mat. **9**(3), 230–232 (1997)
2. P.O. Anikeeva, J.E. Halpert, M.G. Bawendi, V. Bulovic, Nano Lett. **9**(7), 2532–2536 (2009)
3. D. Geißler, C. Würth, C. Wolter, H. Weller, U. Resch-Genger, Phys. Chem. Chem. Phys. **19**(19), 12509–12516 (2017)
4. Q. Wang, K.H. Tran, C. Morin, J. Bonnety, G. Legros, P. Guibert, Appl. Phys. B **123**(199), 1–14 (2017)
5. H. Moon, C. Lee, W. Lee, J. Kim, H. Chae, Adv. Mat. **31**(34), 1804294 (2019)
6. S.W. Buckner, R.L. Konold, P.A. Jelliss, Chem. Phys. Lett. **394**(4–6), 400–404 (2004)
7. M. Tata, S. Banerjee, V.T. John, Y. Waguespack, G.L. Mcpherson, Colloids Surf. A: Physicochem. Eng. Aspects **127**(1–3), 39–46 (1997)
8. K. Pechstedt, W. Tracy, B. Jeremy, T. Melvin, J. Phys. Chem. C **114**(28), 12069–12077 (2010)
9. C. Cheng, H. Yan, Phys. E **41**(5), 828–832 (2009)
10. J. Pengtao, J. Zheng, M. Ikezawa, X. Liu, S. Lv, X. Kong, J. Zhao, Y. Masumoto, J. Phys. Chem. C **113**(31), 13545–13550 (2009)
11. H.S. Heo, J.H. Jo, S.J. Lee, C. Yun, S.-H. Choi, J.H. Lee, K. Lee, Chem. Mater. **34**(15), 6637–7094 (2022)
12. M.J. Smith, S.T. Malak, J. Jung, Y.J. Yoon, C.H. Lin, S. Kim, K.M. Lee, R. Ma, T.J. White, T.J. Bunning, Z. Lin, V.V. Tsukruk, ACS Appl. Mater. Interfaces **9**(20), 17435–17448 (2017)
13. G. Khanarian, Opt. Eng. **40**(6), 1024–1029 (2001)
14. S. Baek, S. Kim, J.Y. Noh, J.H. Heo, S.H. Im, K.-H. Hong, S.-W. Kim, Adv. Opt. Mater. **6**(15), 1800295 (2018)
15. G. Wypych Handbook of Polymers, Elsevier (2012)
16. S.A. Stern, J. Membrane. Sci. **94**, 1–65 (1994)
17. J.P. Park, J.-J. Lee, S.-W. Kim, Sci. Rep. **6**(1), 30094 (2016)
18. E.-P. Jang, J.-H. Jo, M.-S. Kim, S.-Y. Yoon, S.-W. Lim, J. Kim, H. Yang, RSC Adv. **8**(18), 10057–10063 (2018)
19. C. Yoon, K.P. Yang, J. Kim, K. Shin, K. Lee, Chem. Eng. J. **382**, 122792 (2020)
20. D. Geißler, N. Hildebrandt, Anal. Bioanal. Chem. **408**(17), 4475–4483 (2016)
21. M.C. Dos Santos, W.R. Algar, I.L. Medintz, N. Hildebrandt, Chem. **125**, 115819 (2020)
22. I. Medintz, A. Clapp, H. Mattoussi, E.R. Goldman, B. Fisher, J.M. Mauro, Nature Mater. **2**(9), 630–638 (2003)
23. Z. Meng, K. Fu, Y. Zhao, Y. Zhang, Z. Wei, Y. Liu, X. Ren, Z.-Q. Yu, J. Mater. Chem. C **8**, 1010–1016 (2020)
24. M. Noh, T. Kim, H. Lee, C.-K. Kim, S.-W. Joo, K. Lee, Colloids Surf. A: Physicochem. Eng. Aspects **359**, 39–44 (2010)
25. M. Sykora, A.Y. Koposov, J.A. McGuire, R.K. Schulze, O. Tretiak, J.M. Pietryga, V.I. Klimov, ACS Nano **4**, 2021–2034 (2010)
26. K.F. Chou, A.M. Dennis, Sensors **15**(6), 13288–13325 (2015)
27. D. Abu Saleh, A. Sosnik, Nanotechnology **32**(19), 195104 (2021)
28. T. Kang, K. Um, J. Park, H. Chang, D.C. Lee, C.-K. Kim, K. Lee, Sens. Actuator B-Chem. **222**, 871–878 (2016)
29. P.S. Nunes, P.D. Ohlsson, O. Ordeig, J.P. Kutter, Microfluid. Nanofluid. **9**, 145–161 (2010)
30. H.S. Jang, H. Yang, S.W. Kim, J.Y. Han, S.-G. Lee, D.Y. Jeon, Adv. Mater. **20**(14), 2696–2702 (2008)